Observation of an index-of-refraction-induced change in the Drude parameters of Ag films

H. Gugger,* M. Jurich, and J. D. Swalen
IBM Research Laboratory, San Jose, California 95193

A. J. Sievers
Laboratory of Atomic and Solid State Physics and Materials Science Center, Cornell University, Ithaca, New York 14853

(Received 29 December 1983; revised manuscript received 13 April 1984)

The method of attenuated total internal reflection has been used in the visible region to obtain precise values of the dielectric function of Ag films in contact with different dielectric media. By measuring, at eight visible laser wavelengths, the surface-plasmon resonance of an Ag film against air and then against an organic liquid, we show that for both cases the dielectric function can be described by the Drude model with the well-known frequency-dependent relaxation time, namely, $\tau^{-1}(\omega)=\tau_0^{-1}+\beta\omega^2$. The interesting results are that $\tau_0^{-1}(\text{liquid})>\tau_0^{-1}(\text{air})$, that $\beta(\text{liquid})<\beta(\text{air})$, and that the plasma frequency $\omega_p(\text{liquid})>\omega_p(\text{air})$. The fact that β changes—the sign of the change or its magnitude—appears to eliminate all previous models which have been proposed to describe this frequency-dependent term. The observed changes in β and ω_p are consistent with the idea of a complex relaxation time whose real and imaginary parts are connected in a causal way. The index-of-refraction dependence of the Drude parameters demonstrates that surface electrodynamics must play an important role. The observed trends reported here could be accounted for if increasing the index of the dielectric half-space would increase the attractive surface-plasmon interaction and decrease the magnitude of electron-electron scattering in the Ag surface.

I. INTRODUCTION

The optical data for the noble metals at frequencies below the interband absorption edge are accurately characterized by the free-electron Drude model.[1] The real and imaginary parts of the metal dielectric function can be written as

$$\epsilon_1 \simeq \epsilon_\infty - \frac{\omega_p^2}{\omega^2} \tag{1}$$

and

$$\epsilon_2 = \frac{\epsilon_\infty - \epsilon_1}{\omega\tau} \tag{2}$$

in the limit where $\omega\tau \gg 1$. The three parameters of the model are ϵ_∞, the core polarizability and interband contribution to the dc dielectric constant, $\omega_p^2 = 4\pi Ne^2/m$, the plasma frequency squared, and τ^{-1}, the electron scattering rate. For the noble metals, this scattering rate has the form[1]

$$\tau^{-1} = \tau_0^{-1} + \beta\omega^2 \, . \tag{3}$$

Both τ^{-1} and to a lesser extent ω_p are found to vary depending on the sample preparation techniques.[2,3] The source of these variations remains poorly understood.

Because annealing thin-film Au samples[2] decreases the size of β, an inhomogeneous medium model composed of crystalline grains and disordered intergranular material has been used with a two-carrier Drude model to account for the quadratic dependence of the relaxation time.[4] However, it is unlikely that the nonzero β observed for single-crystal bulk samples[5] also can be explained in this manner. The possibility that the frequency-dependent term stems from electron-electron scattering has been considered in some detail by Christy and co-workers.[6,7] They have not been able to obtain quantitative agreement with the electron-electron contribution inferred from the measured electrical and thermal resistivities. Recently, Smith and Ehrenreich[8] have proposed that this frequency dependence follows from a more precise estimate of the electron-phonon interaction. Their numerical estimate of the β's are in reasonable agreement with the room-temperature experimental values.

A consistent explanation of the variations observed for ω_p has not yet been found although the changes are usually assigned to surface morphology. The ω_p's measured for the thin semitransparent Au films investigated by Théye are about 5% larger than the values reported for electropolished bulk samples.[2] Almost the same change in ω_p has been measured by Hodgson for the internal and external surface of an opaque Au film[9] with the larger ω_p occurring for the film-substrate interface. By studying surface-plasmon resonance excitation at both surfaces of evaporated metal films, Weber and McCarthy confirmed the Au results and showed that a similar effect existed for Ag films.[10,11] They found that the ω_p at the substrate interface was consistently about 5% larger than ω_p at the air interface, independent of the growth rate of the film which was varied over a factor of 100. They also proposed that this difference could be understood if the Ag film density near the air surface was several percent below that near the substrate interface.

To date, both the relaxation rate and the plasma frequency of the noble metals have been treated as independent quantities, although in general, if τ depends on fre-

quency, so must ω_p.[12–15] This interrelation between the frequency dependences of the two Drude model parameters has been demonstrated in a detailed analysis of the phonon-assisted absorption process.[13] The two frequency-dependent Drude model parameters $\omega_p(\omega)$ and $\tau(\omega)$ are given by

$$[\omega_p(\omega)]^2=\frac{\omega_p^2}{1+\bar{\lambda}(\omega)} \tag{4}$$

and

$$\tau(\omega)=\bar{\tau}(\omega)[1+\bar{\lambda}(\omega)]\,, \tag{5}$$

where the frequency dependence of $\bar{\lambda}(\omega)$ is intimately related to the Kramers-Kronig transform of $[\omega\bar{\tau}(\omega)]^{-1}$.

One analysis of the infrared and optical properties of the alkali metals has been made[15] which makes use of expressions similar to Eqs. (4) and (5). An intrinsic surface-plasmon-assisted absorption process was proposed to account for the enhanced infrared mass. It is a Holstein-type process with the surface plasmons taking the role of the phonons. One of the predictions of the surface-plasmon-assisted absorption model is that both Drude parameters of the metal should depend on the dielectric constant of the neighboring substrate. Consequently, the observed variations in the optical properties of the noble-metal films could be a function of the index of refraction of the dielectric substrate as well as surface morphology. One purpose of this paper is to report on our experimental test of this possibility.

By using liquid dielectrics together with the surface-plasmon resonance technique, we have measured the change in the dielectric function of Ag films with a constant surface structure as a function of the interface dielectric constant. The previously reported change[10] in plasma frequency between Ag-glass and Ag-air interfaces is reproduced in our experiments. When liquids with various refractive indices are placed on the same surface where Ag-air measurements were made, β is observed to decrease consistent with a decrease in the mass parameter (an increase in ω_p).

The fact that β changes at all in our experiments is not compatible with the usual assignment to electron-electron[7] or electron-phonon[8] processes. In addition, mechanisms which rely on metal grains,[4] surface roughness, a reduced film density near the air interface,[11] or surface-plasmon-assisted absorption[15] cannot account for the observed increase in ω_p. However, the dielectric constant dependence of the experimental results demonstrates that the Drude model parameters are controlled by a surface process in which electrodynamics plays an important role. The sign of the effect is consistent with the dielectric reducing the first moment of the induced surface charge and hence reducing the size of the electron-hole excitation term, or with a dielectric enhanced surface-plasmon interaction reducing the magnitude of the surface electron-electron scattering term.

In the next section, the attenuated total internal reflection apparatus and experimental measurements are described. The Ag-air and Ag-liquid interface results are presented in Sec. III. We demonstrate in Sec. IV that the experimental data are consistent with the dielectric induced change in both the frequency-dependent scattering rate and the electron mass.

II. EXPERIMENTAL DETAILS

A. Attenuated total internal reflection (ATR) apparatus

We have used surface-plasmon resonance excitation at a number of laser wavelengths to determine the dielectric function of Ag in the visible regions.[16] The attenuated total reflection setup is shown in Fig. 1.

Reflectivity measurements were done with the prism mounted on a computer-controlled rotating table to scan the angle of incidence and collect the digitized data. The wavelengths used were from an argon-ion laser (488.0 and 514.5 nm), from a krypton-ion laser (530.9, 568.2, 647.1 and 676.4 nm), from a helium-neon laser (632.8 nm), and from a helium-cadmium laser (441.6 nm). To achieve better rejection of the light with the unwanted polarization, two Glan-Thompson prism polarizers were placed sequentially in front of a Fresnel rhomb.

Since the surface-plasmon resonance occurs exclusively upon excitation with TM waves, the correct angle of polarization was set by rotating the rhomb to a minimum reflection for TM light, i.e., at the angle of maximum plasmon absorption. The coated prism was positioned in such a way that the chopped laser beam always refracted to the center portion of the film to minimize beam walk. The reflected signal at twice the angle was detected with a p-i-n photodiode. A fraction of the chopped laser beam was split off before the prism with a pellicle beam splitter to serve as the laser intensity reference. Both signals, the reflection and the laser reference signal, were separately detected and amplified; their ratio gave the final output.

B. Procedure

The Ag films, approximately 500 Å thick, were vacuum deposited onto the base of LaSF31 Schott glass isosceles prisms at a rapid rate (50–100 Å/s) to obtain a fine grained surface. Prisms with apex angles of 53° or 57° were used so that the critical angle of the glass/air interface could be observed.

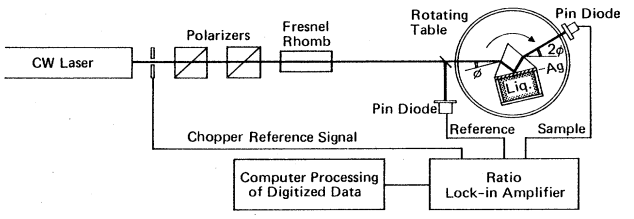

FIG. 1. Schematic diagram of experimental apparatus. A Teflon cup containing air or liquid was pressed with a split o-ring onto the silver film on the base of a high-refractive-index prism. Two Glan-Thompson prism polarizers were used to improve rejection of light of the other polarization. Rotation of the Fresnel rhomb allowed conversion between s and p polarizations. The rotating table included an arm at 2ϕ to track the reflected beam.

We measured the angles of each prism by differences in the angles of back reflection. Then we determined the refractive index of the prisms by comparing the results from different methods.

(1) The glass-melt information sheet[17] for our Schott glass (LaSF31) prisms gave the refractive index at selected wavelengths and constants for a power-series expansion of the dispersion curve. These data were then used to calculate the refractive indices at our laser wavelengths.

(2) From a measurement of a critical angle θ_c, the refractive index can be calculated from Snell's law.

(3) From the minimum angle of deviation measured for the prism and knowing the prism angle, the refractive index was calculated.[18]

Since all three values agreed within experimental error at all wavelengths, we decided to use the easily calculated values from the Schott data.

The prism angle was checked at each wavelength by the critical angle for the glass-air interface. Standard deviations for these determinations using eight wavelengths were typically $\pm 0.005°$. From the prism index and prism angle, the index of refraction of the liquid n could then be calculated from the experimentally observed change in critical angle θ_c when a liquid replaces air without any further experiments. Since n is a function of, e.g., wavelength, purity, and temperature, this procedure directly gave the index for our experimental conditions.

The first measurement for every freshly coated silver film was an ATR experiment at the silver-air interface to determine the dielectric constants of bare silver at all wavelengths under investigation, as well as the thickness of the film. This measurement was to identify any differences in the dielectric function of Ag that might arise from surface morphology. Then, carbon tetrachloride ($n \sim 1.46$) or hexane ($n \sim 1.37$) were placed next to the Ag and the dielectric constants at the Ag-liquid interface were determined. In Fig. 2, the angular location of the critical angle is shown for a typical ATR curve at a silver-hexane interface, with the critical angle being essentially that for hexane-glass.

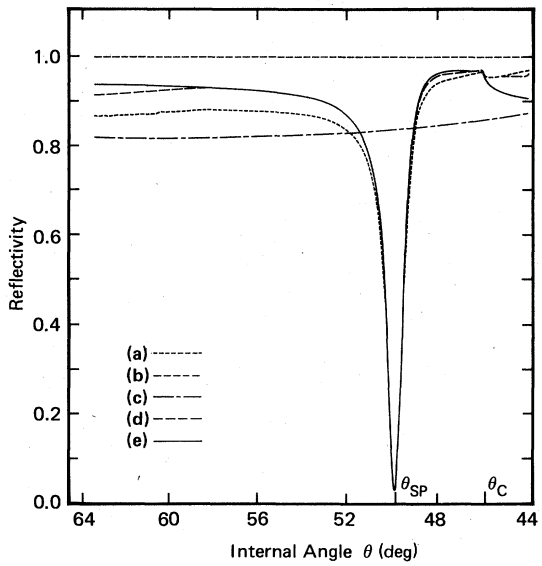

FIG. 2. Typical reflectivity curve as a function angle. For this example, hexane is adjacent to Ag. θ_{SP} is the reflectivity minimum at the surface-plasmon angle and θ_c is the critical angle of air or liquid and the prism. Curves: (a) experimental curve; (b) prism absorption loss; (c) prism reflection loss from both faces; (d) experimental curve corrected for absorption, reflections, and background; (e) calculated "best fit" of the Fresnel equations.

III. RESULTS

The values of the complex dielectric function of Ag were calculated by a least-squares fit of the exact Fresnel reflection formulas to the experimental ATR curves. The matrix procedure outlined by Heavens[19] was used to calculate the reflectivity for a layered structure. From the experimental reflectivity curves for the Ag-air interface, we determined ϵ_1 and ϵ_2 for each wavelength and the thickness of the film. When the liquid was introduced, we again used a least-squares-fitting procedure to obtain ϵ_1 and ϵ_2, but now the thickness of the Ag film was set equal to the average value determined for the Ag-air-interface measurement. The measured values for the films are listed in Table I.

Initially, the calculated reflectivity curves deviated significantly from the experimental ones. Searching for sources of this deviation, it was determined that at least four factors contribute: (1) reflection losses at each face of the prism, (2) absorption from transmission through the prism, especially at short wavelengths, (3) movement of the beam from one section to another section of the film with slightly different optical properties as the prism is rotated, and (4) dark current of the measurement system. In order to correct for these deviations, we collected both TE and TM ATR data from which we subtracted

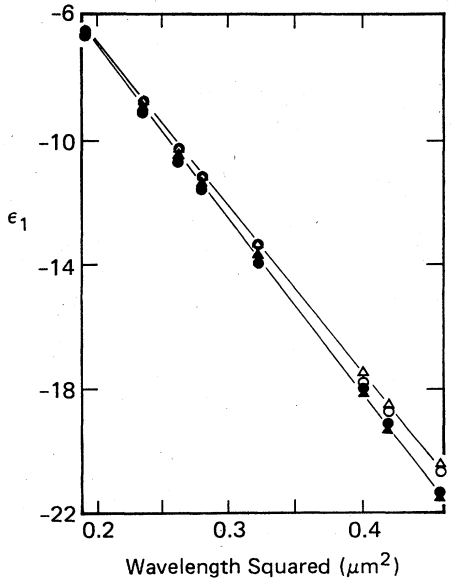

FIG. 3. Measured real part of the dielectric function of silver versus wavelength squared for both air △ and CCl_4 ▲ half-spaces and air ○ and hexane ● half-spaces. The lines are average values and given to clearly show the trends.

TABLE I. Experimentally determined dielectric function of Ag and related optical parameters. (Straight line shown in Fig. 4 without the point of 4416 Å because it is more than three standard deviations from the line.)

	Liquid			Air		
λ (Å)	ϵ_1	ϵ_2	τ_e^{-1} (10^{14} s^{-1})	ϵ_1	ϵ_2	τ_e^{-1} (10^{14} s^{-1})
CCl_4			$d=58.4\pm0.4$ nm			
4416	−6.471	0.4191	1.634	−6.323	0.4755	1.953
4880	−9.087	0.5139	1.463	−8.772	0.5243	1.577
5145	−10.528	0.6239	1.523	−10.265	0.6074	1.552
5309	−11.486	0.6547	1.456	−11.150	0.6387	1.490
5682	−13.834	0.7855	1.423	−13.374	0.7003	1.332
6328	−17.940	1.0091	1.340	−17.452	0.9599	1.329
6571	−19.334	1.0537	1.289	−18.582	0.9473	1.218
6764	−21.448	1.2074	1.298	−20.487	1.0270	1.165
Hexane			$d=37.4\pm0.1$ nm			
4416	−6.6037	0.4464	1.761	−6.567	0.3549	1.416
4880	−9.122	0.4739	1.3721	−8.749	0.4098	1.229
5145	−10.606	0.5452	1.347	−10.230	0.4524	1.154
5309	−11.609	0.5752	1.290	−11.155	0.4785	1.111
5682	−13.922	0.6808	1.245	−13.385	0.5570	1.055
6328	−18.129	0.9657	1.287	−17.772	0.7140	0.971
6471	−19.133	0.9513	1.187	−18.701	0.7492	0.956
6764	−21.409	1.0408	1.132	−20.650	0.8073	0.908

the dark current from each. In the prism, absorption losses were very small because of the relatively long wavelength and good transmission quality of the high-index glass. Hence we used the measured TE data to calculate a correction curve for absorption losses after correcting for its reflection losses. These absorption corrections including those for TM reflection losses were then applied to the TM curves. The various reflectivity and correction curves are shown in Fig. 2. Note the close agreement between the corrected experimental curve and the calculated curve, indicating the precision with which the values of the dielectric function given in Table I describe the experimental measurements.

In Fig. 3 we plot our experimental values for the real part of the dielectric function of silver versus wavelength squared for both the air-silver and liquid-silver cases. Two different liquids have been studied, CCl_4 and hexane. The values for $\omega_{p,e}^2$ and ϵ_∞ were obtained from a least-squares fit to an ϵ_1-versus-λ^2 line for both the Ag-air and Ag-liquid data. These derived experimental numbers are recorded in Table II.

The inverse relaxation time from the experimental values for ϵ_1 and ϵ_2 at each frequency is obtained from

$$\tau_e^{-1}=\frac{\omega\epsilon_2}{\epsilon_\infty-\epsilon_1}\ . \tag{6}$$

Figures 4(a) and 4(b) show a plot of τ_e^{-1} versus ω^2 for Ag in contact with CCl_4 and hexane, respectively. To a good approximation, these data can be fitted by Eq. (3). The values of τ_0^{-1} and β obtained from a least-squares fit to these data are given in Table II.

IV. DISCUSSION

The experimental results clearly show that the effective dielectric function of the metal is changed when liquid replaces air. Could these results be explained by surface roughness on the Ag film? A metal-insulator composite layer is often used to model the optical properties of a roughened surface.[10,20] According to the Maxwell-Garnett theory, a Lorenz-Lorentz type of dispersion will occur in such a layer. We find that replacing a 100-Å-

TABLE II. Experimentally determined Ag Drude model parameters.

	Film no. 1		Film no. 2	
	Air	CCl_4	Air	Hexane
ϵ_∞	4.07±0.08	4.47±0.11	4.14±0.08	4.22±0.06
$\omega_{p,e}^2$ (eV)	9.10±0.02	9.33±0.03	9.14±0.02	9.27±0.02
τ_0^{-1}(10^{13} s^{-1})	6.4 ±0.9	10.5 ±0.5	5.5 ±0.5	9.61±0.32
β_0 [10^{12} $s^{-1}(eV)^{-2}$]	16.1 ±1	7 ±2	11 ±1	6 ±1
λ_0 (10^{-2})	9.8 ±3	4.5 ±1.4	7.5 ±2.4	4.5 ±1.4
α^{-1} (eV)	9 ±4	9 ±4	11 ±4	11 ±4
ω_p (eV)	9.5 ±0.1	9.5 ±0.1	9.5 ±0.1	9.5 ±0.1

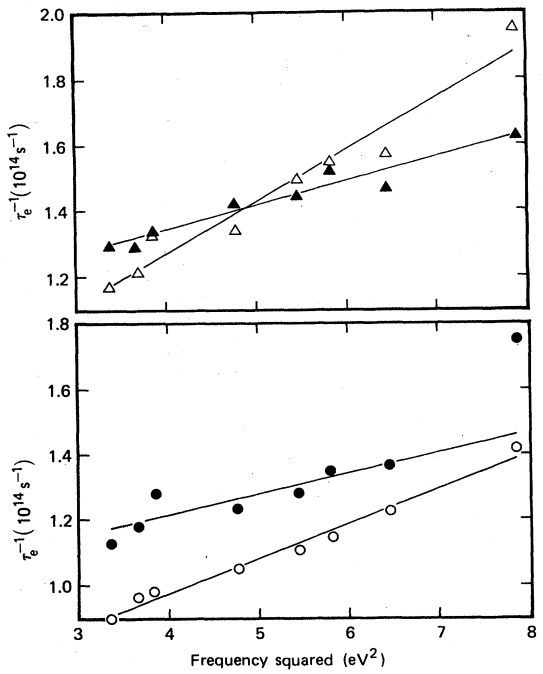

FIG. 4. Relaxation time calculated from the measured values of dielectric function of silver with Eq. (6), as a function of energy squared: (a) air △, CCl_4 ▲, and (b) air ○, hexane ●.

thick composite Ag-air layer on a silver film with a Ag-liquid composite layer of the same thickness causes the predicted ATR minimum at the Ag-liquid interface to shift to increasing internal angles corresponding to a less negative real part of the dielectric function. (Our measured shift is always to *decreasing* internal angles with respect to the predicted ATR minimum at the Ag-liquid interface from the Ag-air data.) Hence, although it is possible to account for the air-Ag results by adjusting the parameters in the Maxwell-Garnett model, once these parameters are fixed, the model cannot account for the liquid-Ag data. Inspection of the data in Fig. 3 and Table I shows that for both films a composite medium layer would be expected to produce the opposite effect on the real part of the dielectric function to what is observed experimentally. In addition, Maxwell-Garnett theory implies that the largest influence should be at short wavelengths close the sphere resonance condition, but experimentally the largest percentage change in ϵ_1 is observed in the long-wavelength region.

Another possibility is the two-carrier model for crystallites (a) and grain boundaries (b) proposed by Nagel and Schnatterly.[4] For the limit $\omega\tau_a > 1$, $\omega\tau_b \ll 1$, and $(2N_b/N_a)\ \omega^2\tau_b^2 \ll 1$, they find an effective relaxation time which is frequency dependent, namely,

$$\tau^{-1}=\tau_a^{-1}+\frac{N_b}{N_a}\tau_b\omega^2 . \tag{7}$$

In this expression, τ_a is due to scattering from phonons in crystallites while τ_b is very much smaller and is presumably controlled by the thickness of the grain boundaries. N_b/N_a is the ratio of the average grain size to the average crystallite size.

In Table II it is seen that the frequency-independent contribution (τ_0^{-1}) to the relaxation time increases by about a factor of 2 when air is replaced by a liquid. The mechanical modulation of the metal surface by the thermal fluctuations in the liquid could account for this observation; hence in Eq. (7) an increase in τ_a^{-1} is to be expected. Since τ_b^{-1} is already larger than the optical probing frequency, the thermal fluctuations in the liquid should not have much effect on the grain-boundary relaxation times, certainly nothing like the factor of 2 observed for β of Table II. On these grounds, the two-carrier model can be eliminated as the source of the frequency-dependent relaxation time.

The change in β observed for the air-liquid substitution is not compatible with relaxation mechanisms which rely solely on bulk processes. Identification with the usual electron-electron or electron-phonon scattering now seems unlikely.

We now demonstrate that the measured change in the optical constants are consistent with a dielectric induced change both in the electron frequency-dependent scattering rate and in the optical mass. If we define the complex frequency-dependent electron scattering rate as

$$\hat{\tau}^{-1}=\hat{\Gamma}=\Gamma_1+i\Gamma_2 , \tag{8}$$

and for later convenience set $\Gamma_2 \equiv -\omega\lambda$, then the Drude expressions become

$$\epsilon_\infty-\epsilon_1(\omega)=\frac{\omega_p^2}{\Gamma_1^2}(1+\lambda)\left[\left[\frac{\omega}{\Gamma_1}\right]^2(1+\lambda)^2+1\right]^{-1} \tag{9}$$

and

$$\epsilon_2(\omega)=\frac{\omega_p^2}{\omega\Gamma_1}\left[\left[\frac{\omega}{\Gamma_1}\right]^2(1+\lambda)^2+1\right]^{-1} . \tag{10}$$

The experimental relaxation frequency is

$$\tau_e^{-1}=\frac{\omega\epsilon_2(\omega)}{\epsilon_\infty-\epsilon_1(\omega)}=\Gamma_1(1+\lambda)^{-1} \tag{11}$$

and the experimental plasma frequency squared is

$$\omega_{p,e}^2\approx\omega^2[\epsilon_\infty-\epsilon_1(\omega)]=\omega_p^2(1+\lambda)^{-1} . \tag{12}$$

The quadratic frequency dependence observed for the electron scattering rate in noble metals can be modeled if $\hat{\Gamma}$ is taken to have the following approximate causal form:

$$\Gamma_1=\Gamma_d+\lambda_0\omega^2\alpha(1+\omega^2\alpha^2)^{-1} \tag{13}$$

and

$$\lambda=\lambda_0(1+\omega^2\alpha^2)^{-1} . \tag{14}$$

Then

$$\Gamma_1=\Gamma_d+\beta\omega^2 , \tag{15}$$

where

$$\beta=\alpha\lambda . \tag{16}$$

In the limit that $\lambda \ll 1$, Eq. (11) shows that Γ_1 is a good approximation to τ_e^{-1}. For the limit $\alpha\omega \ll 1$ which we as-

sume in the analysis of the data below $\lambda \rightarrow \lambda_0$ and $\beta \rightarrow \beta_0$, so both parameters are frequency independent and the real part of the relaxation rate contains a pure quadratic term.

The second assumption which we introduce is that α is independent of the presence of the dielectric half-space. This assumption is reasonable since even if α^{-1} is related to the electrostatic surface-plasmon mode frequency in Ag, this mode is pinned at a fixed frequency, by the high-frequency interband transitions, independent of the dielectric index of refraction.

The subscripts l and a are used to distinguish between the measured Ag-liquid and Ag-air interface results. From Eq. (16)

$$\frac{\beta_{a0}}{\beta_{l0}} = \frac{\lambda_{a0}}{\lambda_{l0}} \tag{17}$$

and from Eq. (12)

$$\frac{(\omega_{p,e}^2)_l}{(\omega_{p,e}^2)_a} = \frac{1+\lambda_{a0}}{1+\lambda_{l0}} . \tag{18}$$

These two experimental numbers enable us to determine both λ_{a0} and λ_{l0} which are presented in Table II for both films. The measured value for β_{a0} is then used to estimate α^{-1}. This parameter value which is consistent with the $\omega\alpha \ll 1$ assumption is remarkably close to the value of the Ag plasma frequency.

A consistent set of parameters λ_{a0}, λ_{l0}, and α^{-1} is found which describes the frequency-dependent relaxation time represented by Eqs. (13) and (14). The good agreement between experiment and this phenomenological model over the visible region demonstrates that the change in the optical properties is due to a dielectric induced change in the electron relaxation time. Somewhat surprising is the sign of the change.

For the alkali metals it has been shown that a surface-plasmon-assisted photon absorption mechanism[15] which leads to an initial ω^4 dependence of the Drude scattering rate is consistent with the experimental data if the magnitude of the mechanism is used as a free parameter. It was also shown that increasing the index of refraction of the neighboring dielectric half-space increases the strength of this term, increases λ, and hence *decreases* ω_p. The fact that the optical properties of the noble metals change in the opposite way when the index of refraction is increased is a clear indication that this mechanism cannot be the dominant factor here.

It has been known for some time that when a metal surface is probed with TM polarized radiation, electron-hole (e-h) pair excitation should contribute to the optical absorption.[21–23] Recently, Ljungbert and Apell[24] have proposed that this effect can be described in terms of a single parameter, the first moment of the induced surface charge of the metal. From their calculation of the relative contribution of electron-hole pairs to the total absorptance, we can estimate the magnitude of the appropriate frequency-dependent scattering rate which describes this process. For $\omega \ll \omega_p$, we find[24]

$$\tau_{e\text{-}h}^{-1} \simeq \frac{\omega^2}{c} |\operatorname{Re} d_\perp(0)| , \tag{19}$$

where $|\operatorname{Re} d_\perp(0)|$ is the center of gravity of the induced charge which is measured with respect to the edge of the positive metal background. Although the magnitude of this relaxation term is estimated from Ref. 24 to be less than 4% of the strength needed to explain the data in Table II, it does have the correct frequency dependence. Moreover, because of the Pauli exclusion principle, the quantity $|\operatorname{Re} d_\perp(0)|$ for a liquid-metal interface should be smaller than $|\operatorname{Re} d_\perp(0)|$ for an air-metal interface. It is not clear to us, though, how this parameter could change by the measured factor of 2 observed for β (see Table II).

The large change in β required for the electron-hole excitation mechanism leads us to speculate on another possibility which again makes use of surface plasmons but now in an indirect role. The fact that the optical properties of the alkali metals and noble metals seem to change in opposite ways when the index of refraction of the half-space changes may be simply an indication of the size of the electron-electron scattering term within the skin depth of each metal type. Inkson[25] has pointed out that although the surface-plasmon interaction itself is attractive below the electrostatic mode limit, the decrease in the bulk-plasmon exchange interaction near the surface causes the total interaction for quasiparticles to be more repulsive than in the bulk.

If, below the electrostatic mode frequency, electron-electron scattering dominates the surface-plasmon-mediated scattering within a skin depth for the noble metals while the converse is true for the alkali metals, then a consistent picture emerges. Increasing the index of the dielectric half-space would increase the strength of the attractive surface-plasmon interaction for both metal types and decrease the magnitude of the electron-electron scattering term within a skin depth, but this decrease would only be apparent in the optical properties of the noble metals.

Although it has been known for many years that the Drude parameters of noble-metal films depend on surface morphology and many relaxation processes have been invoked to explain the quadratic frequency dependence of the electron relaxation frequency, it was not generally recognized that surface electrodynamics could play an important role at such low frequencies. Our systematic study of an index-of-refraction induced change in the Drude parameters of Ag films demonstrates that this is the case. More experiments need to be carried out to identify the physical process, but the general conclusion is now clear: The dielectric function required to describe the ir and optical properties of a noble-metal mirror depends on the dielectric constant of the adjoining medium.

ACKNOWLEDGMENTS

One of us (H.G.) acknowledges support by IBM. The initial work by A. J. Sievers was supported by the NSF under the Visiting Scientist program. Continuing support has been obtained from the National Science Foundation under Grant No. DMR-81-06097 and from U.S. Air Force Office of Scientific Research under Grant No. AFOSR-81-0121B.

*Permanent address: Ciba-Geigy AG, KA Forschungszentrum, CH-1701 Fribourg, Switzerland.
[1]P. O. Nilsson, in *Solid State Physics,* edited by H. Ehrenreich, F. Seitz, and D. Turnbull (Academic, New York, 1974), Vol. 29, pp. 218—221.
[2]M. L. Théye, Phys. Rev. B **2**, 3060 (1970).
[3]M. M. Dujardin and M. L. Théye, J. Phys. Chem. Solids **32**, 2033 (1971).
[4]S. R. Nagel and S. E. Schnatterly, Phys. Rev. B **9**, 1299 (1974).
[5]S. Roberts, Phys. Rev. **118**, 1509 (1960).
[6]R. T. Beach and R. W. Christy, Phys. Rev. B **16**, 5277 (1977).
[7]G. R. Parkins, W. E. Lawrence, and R. W. Christy, Phys. Rev. B **23**, 6408 (1981).
[8]J. B. Smith and H. Ehrenreich, Phys. Rev. B **25**, 923 (1982).
[9]J. N. Hodgson, J. Phys. Chem. Solids **29**, 2175 (1968).
[10]W. H. Weber and S. L. McCarthy, Appl. Phys. Lett. **25**, 396 (1974).
[11]W. H. Weber and S. L. McCarthy, Phys. Rev. B **12**, 5643 (1975).
[12]T. Holstein, Ann. Phys. (N.Y.) **29**, 410 (1964).
[13]P. B. Allen, Phys. Rev. B **3**, 305 (1971).
[14]J. W. Allen and J. C. Mikkelsen, Phys. Rev. B **15**, 2952 (1977).
[15]A. J. Sievers, Phys. Rev. B **22**, 1600 (1980).
[16]I. Pockrand, Surf. Sci. **72**, 577 (1978).
[17]Schott Glass Co. (private communication).
[18]M. Born and E. Wolf, *Principles of Optics* (Pergamon, Oxford, 1980), pp. 177—181.
[19]O. S. Heavens, *Optical Properties of Thin Solid Films* (Dover, New York, 1965), pp. 69—74.
[20]G. J. Kovacs, in *Electromagnetic Surface Modes,* edited by A. D. Boardman (Wiley, New York, 1982), p. 143.
[21]P. J. Feibelman, Phys. Rev. B **14**, 762 (1976).
[22]K. L. Kliewer, Phys. Rev. B **14**, 1412 (1976).
[23]P. J. Feibelman, Prog. Surf. Sci. **12**, 287 (1983).
[24]A. Ljungbert and P. Apell, Solid State Commun. **46**, 47 (1983).
[25]J. C. Inkson, J. Vac. Sci. Technol. **11**, 943 (1974).